

Title: Ecological succession and viability of human-associated microbiota on restroom surfaces

Running Title: Longitudinal Analysis of the Restroom Microbiome

Sean M. Gibbons^{1,2*}, Tara Schwartz^{3*}, Jennifer Fouquier^{3,4}, Michelle Mitchell³, Naseer Sangwan², Jack A. Gilbert^{2,5,6,7,8}, Scott T. Kelley³

¹Graduate Program in Biophysical Sciences, University of Chicago, Chicago, IL 60637, U.S.A.

²Institute for Genomic and Systems Biology, Argonne National Laboratory, 9700 South Cass Avenue, Argonne, IL 60439, U.S.A.

³Department of Biology, San Diego State University, 5500 Campanile Drive, San Diego, CA 92182, U.S.A.

⁴Graduate Program in Bioinformatics and Medical Informatics, San Diego State University, 5500 Campanile Drive, San Diego, CA 92182, U.S.A.

⁵Department of Ecology and Evolution, University of Chicago, 1101 E 57th Street, Chicago, IL 60637

⁶Marine Biological Laboratory, 7 MBL Street, Woods Hole, MA 02543, USA

⁷College of Environmental and Resource Sciences, Zhejiang University, Hangzhou, 310058, China

⁸Corresponding Author: gilbertjack@anl.gov; (630) 915-2383

*These authors contributed equally to the work presented in this manuscript

Abstract

Human-associated bacteria dominate the built environment (BE). Following decontamination of floors, toilet seats, and soap dispensers in 4 public restrooms, *in situ* bacterial communities were characterized hourly, daily, and weekly to determine their successional ecology. The viability of cultivable bacteria, following the removal of dispersal agents (humans), was also assessed hourly. A late successional community developed within 5-8 hours on restroom floors, and showed remarkable stability over weeks to months. Despite late successional dominance by skin- and outdoor-associated bacteria, the most ubiquitous organisms were predominantly gut-associated taxa, which persisted following exclusion of humans. *Staphylococcus* represented the majority of the cultivable community, even after several hours of human-exclusion. MRSA-associated virulence genes were found on floors, but were not present in assembled *Staphylococcus* pan-genomes. Viral abundances, which were predominantly enterophage, human papilloma and herpes viruses, were significantly correlated with bacteria abundances, and showed an unexpectedly low virus-to-bacteria ratio in surface-associated samples, suggesting that bacterial hosts are mostly dormant on BE surfaces.

Importance

We present a detailed longitudinal study of bacterial and viral communities residing on restroom surfaces. Human-associated microbes residing on these surfaces follow rapid and predictable ecological succession from fecal-dominated to skin-dominated communities, and remain viable for many hours. In addition, we show that common opportunistic pathogens, from the genus *Staphylococcus*, dominate the cultivable community for hours after the exclusion of humans.

Introduction

The analysis of microbial diversity of indoor environments, collectively termed the Built Environment (BE), is important because of its potential impact on human health. It is estimated that humans in industrialized countries spend as much as 90% of their lives indoors (1, 2). Indeed, for billions of humans, the “great indoors” comprises the new human ecosystem. BEs contain an enormous variety of potential microhabitats for microorganisms, and are continually colonized by human and outdoor-associated microbiota (3-5). Understanding the ecological dynamics of the microbiota in BEs may help develop strategies to define and promote an indoor microbiome that minimizes disease risk (2).

While it has long been known that viable bacteria can be cultured from virtually any surface in an indoor ecosystem, we know relatively little about the true diversity and viability of the indoor microbiome. In the past, studies of microbial diversity relied mainly on culture-based techniques (3, 6). However, the application of culture-independent sequencing techniques to the study of BE microbiology has already greatly expanded our understanding of the origin and diversity BE microbes (2).

Comparisons of sequence data collected in one location to other existing datasets generated by the same approaches allows inference of the likely environmental origins of BE communities (e.g., human skin, soil, etc.) (7). Additionally, the impact of season and geographic location on bacterial community composition (5, 8) has revealed an extraordinary variability in BE-associated microbial diversity. However, with a few exceptions, most studies have involved single time-point samplings of surfaces. While this allows for a characterization of microbial diversity, and comparative analysis

between surfaces, replicated time-series studies need to be undertaken in order to understand the formation, stability, and dynamics of BE communities (9). In addition, most BE work has focused on bacterial communities, and there are few studies looking at viral community diversity (2). These are significant gaps that need to be filled in order to understand the distribution and behavior of the microbes that inhabit our BEs.

Restrooms are a shared public space with clear disease transmission potential (4). However, the potential for disease transmission from a surface fomite relies on the accumulation and continued viability of pathogenic taxa. A prior amplicon-sequencing study investigating the biogeography of restroom surfaces established putative colonization sources, gender-specific microbial signatures, and surface-specific community structure for restroom microbial communities (4). This spatial study revealed the dominance of human-associated microbes on restroom surfaces, but did not approach the questions of community assembly dynamics, temporal stability, or viability. In addition, this study focused on bacterial diversity, and did not investigate patterns in viral abundance and diversity. Using a combination of 16S rRNA amplicon sequencing, shotgun metagenomics, culturing, culture-independent bacterial and viral abundance estimates, and building science measurements, we addressed the following questions: What are the successional dynamics of BE microbial communities? How stable are these communities over different timescales? Do we see reproducible assembly of the same microbial community? How and when do different source environments contribute to BE microbial communities? How long do microbes remain viable on BE surfaces, and do we see persistently viable human pathogens? What is the structure and diversity of the surface-associated viral communities, and how does viral abundance relate to bacterial

abundance? And finally, what effects do environmental factors (e.g., temp, humidity, occupancy) have on the diversity and abundance of microbiota? To answer these questions, we characterized the microbial community structure, function, and abundance on floors, toilet seats and soap dispensers over time in 4 restrooms (high use and low use, male and female) following decontamination of each surface. Initially, surfaces were analyzed hourly, and then daily for up to 8 weeks. To determine the influence of humans as a dispersal source, surfaces were sterilized again, and following 4 hours of use, humans were excluded from the restrooms and longitudinal changes in community structure and viability of floor-associated bacterial communities were determined.

Materials and Methods

Sample Collection:

A visual summary of the experimental design, sampling locations, and decontamination results are included in **Figures 1 and S1**. For detailed information about each study, see below.

Eight-Week Study

Samples were collected from three surfaces (the toilet seat, the floor in front of the toilet, and the soap dispenser pump) in two public restrooms on the third floor of the North Life Sciences building at San Diego State University. Samples were collected once a week for an eight-week period between November 22, 2011 and January 31, 2012. For all studies presented in this manuscript, the floor samples were collected from an area beginning directly below the edge of the toilet bowl and extending outwards away from the toilet. Eight hours prior to sample collection each surface was decontaminated using a 10%

bleach solution that was allowed to sit for approximately twenty minutes. After the twenty-minute bleach treatment, the surfaces were rinsed with sterile water (DNA and RNA free molecular grade water). The treated surfaces were shown to be DNA and RNA free by epifluorescence microscopy using SYBR Gold (Invitrogen) staining. Approximately eight hours post decontamination, sterile rayon tipped swabs (MacroPurTM Swab P) that had been moistened with sterile 1X phosphate buffered saline (PBS) were used to obtain surface samples from the targeted restroom surfaces. 50.8 cm x 50.8 cm areas were swabbed for each sample. The entire surface was passed over once with the swab, which took approximately 45 seconds. After surface swabbing, the tips of the swabs were broken off into 1.5 ml microtubes containing 500 µl of sterile 1X PBS solution. The swab tips were then immediately vortexed for ten seconds. 100 µl of solution was removed and fixed in 100 µl of 4% paraformaldehyde for later analysis. The remaining samples were then stored at -20°C until further processing.

Eight-Hour Study

Samples were collected every hour over an eight-hour period from the floor in front of the toilet in two female and two male restrooms in the North Life Sciences Building at SDSU. For sampling purposes, the floor in front of each toilet was partitioned into eight equally sized rectangles to ensure that we did not re-sample the same surface more than once in the eight-hour period. This experiment was conducted on two different days: November 30, 2012 and December 5, 2012 and on two different floors (first and third). The female and male restrooms on the third floor are open to everyone and are used frequently throughout the day. The restrooms on the first floor are locked and reserved for faculty and staff use only, and are used much less frequently. An hour before sample

collection began, the floor in front of each toilet was soaked in 10% bleach for twenty minutes as described above. Once an hour for eight time points, a sterile rayon tipped swab that was moistened with sterile 1X PBS was used to swab one of the eight randomly selected rectangles (25.4 cm x 25.4 cm) on the floor. The entire floor surface was passed over once with the swab, which took approximately 30 seconds. The soap pump handles, and the surfaces of the toilet seats were swabbed, making sure the entire surface was passed over once. Sampling and storage for molecular work and microscopy was performed as described previously. The time-series samples were completed in the four restrooms on the two sampling days.

Month-Long Study

Samples were collected from three restroom surfaces (the toilet seat, the floor in front of the toilet, and the soap dispenser pump) in the same four restrooms used in the eight-hour study every other day beginning January 30, 2013 and ending February 27, 2013. All sampled surfaces were bleach treated as described above the morning of January 30, 2013. This was the only time during the course of this experiment that the restroom surfaces were treated with bleach. The first samples were collected in the afternoon of January 30, 2013. Subsequent samples were collected every other afternoon until February 27, 2013, yielding 15 sampling time points. 50.8 cm x 50.8 cm floor areas were swabbed for each sample. The entire surface was passed over once with the swab, which took approximately 45 seconds. The soap pump handles, and the surfaces of the toilet seats were swabbed, making sure the entire surface was passed over once. Sampling and storage for molecular work and microscopy was performed as described previously.

Human-free study

166 Male and Female, high-use public restroom floors (in front of the toilet seat in two stalls)
167 at San Diego State University were decontaminated as stated above. The restroom floor
168 was cleaned at 8:00 AM, and the restrooms were opened for use as needed for four hours.
169 At 12:00, the restrooms were locked for the remainder of the day to allow for sample
170 collection without restroom use. For sampling purposes, the floor in front of each toilet
171 was partitioned into five equally sized rectangles (25.4 cm x 25.4 cm) to ensure that we
172 did not re-sample the same surface more than once in the eight-hour period. The entire
173 surface was passed over once with the swab, which took approximately 30 seconds.
174 Using aseptic technique, a double tipped CultureSwab (BD, Franklin Lakes, NJ) was
175 dipped in 0.02 μ m filtered 1X PBS and used to collect floor surface samples at 12:00,
176 14:00, 16:00, 18:00, and 20:00 hours. One of the two swabs was broken off into
177 microtubes filled with 500 μ L of 1X PBS to be used for 16S rRNA gene sequencing and
178 for microscopy (as described above). The other swab was broken off into 600 μ L of 0.02
179 μ m filtered 1X PBS to be used later for culturing. After the two microtubes were
180 vortexed, 100 μ L were removed from each 500 μ L tube and added to 100 μ L of 4%
181 paraformaldehyde and later analyzed by microscopy. From each 600 μ L tube intended for
182 culturing, 80 μ L were added to 5 mL of Tryptic Soy Broth (TSB) (BD, Franklin Lakes,
183 NJ) in 15 mL capacity Falcon tubes for culturing at 4 conditions, to mimic room
184 temperature and human body temperature: aerobic 25°C and 37°C, and anaerobic 25°C
185 and 37°C. For the anaerobic conditions, AnaeroGen (Oxoid, Lenexa, KS) packets were
186 used to remove oxygen inside of an airtight jar containing anaerobic samples, and oxygen
187 indicator strips were used to verify the absence of oxygen for the entire culture period.
188 For all samples, including negative and positive controls, the lids were cracked slightly to

189 ensure air exchange as typical for culturing. Aerobic samples were incubated for 2 days,
190 and anaerobic samples were incubated for 4 days. After the incubation period, the
191 samples were stored in a -20°C freezer until they were sent to Argonne National
192 Laboratory for DNA extraction, PCR, and sequencing.

193 *Microscopy*

194 Epifluorescence microscopy was used to ensure that all samples collected contained
195 microbes and VLPs as well as to estimate the abundance of both bacteria and VLPs in
196 each sample. We used methods developed by the Rohwer laboratory (10). Briefly, 100 µl
197 of each of the paraformaldehyde fixed samples collected from restrooms was suspended
198 in 5ml of sterile water, and then filtered onto 0.02 µm Whatman Anodisc filter
199 membranes. The filters were then stained with 1X SYBR Gold for 10 min in the dark
200 before being rinsed and mounted onto slides. The slides were visualized using the Leica
201 microscope at the Electron Microscope Facility at San Diego State University. Image-Pro
202 Plus software was used to record digital images of the slides as well as generate estimates
203 of both bacterial and viral abundance.

204 *Bacterial DNA Extraction*

205 Bacterial DNA was extracted directly from swab tips and residual 1X PBS collection
206 buffer using the PowerSoil DNA Isolation Kit (Mo Bio Laboratories) following the
207 protocol in Flores et al. (2011). The Eight-Hour Study and the One-Month time period
208 used the same protocol, but DNA was extracted using the PowerSoil-htp 96 Well Soil
209 DNA Isolation Kit (Mo Bio Laboratories). Extracted DNA was sent to Argonne National
210 Laboratory for sequencing.

211 *DNA Amplicon and Metagenome Sequencing*

Amplicon sequencing was performed using primers designed to be massively multiplexed and cover the V4-V5 hypervariable region of the 16S rRNA gene using the standard methods outlined by the Earth Microbiome Project (<http://www.earthmicrobiome.org/emp-standard-protocols/16s/>) (11). Samples were sequenced on the Illumina MiSeq platform, at the Argonne National Laboratory core sequencing facility (11). Shotgun-metagenomic sequencing for single-read annotation was performed on 7 surface swab samples (F1FH811302012, F1MH211302012, F3FH412052012, F3FH711302012, F3MH611302012, F3MH811302012, F3MH412052012). Metagenomic libraries were prepared using 1 ng of genomic DNA and the Nextera XT protocol according to manufacturer's instructions (Illumina). Metagenomes were run through the MG-RAST annotation pipeline (12). Shotgun-metagenomes were sequenced for an additional 8 samples (S1Post25A12pmD3, S1Post25A4pmD3, S1Post37A12pmD1, S1Post37A8pmD1, S1Post37A8pmD3, S1Post37An12pmD1, S1Post37An4pmD1, S1Post37An6pmD1) from cultured swabs for genome assemblies. Libraries were prepared as described above.

Sequence analysis

QIIME (v. 1.7.0, Quantitative Insights into Microbial Ecology; www.qiime.org) was used to filter reads and cluster OTUs as described previously (11, 13). Approximately 18% of the ~17 million raw amplicon reads were removed during quality filtering, leaving ~14 million reads for downstream analysis. Briefly, the open reference OTU picking script (pick_open_reference_otus.py) (14) was employed, where sequences were first clustered with the Greengenes (May 2013) reference database (15); OTUs that did not cluster with known taxa (at 97% identity) in the database were then clustered *de novo*. Singleton

sequences were removed prior to downstream analyses. Representative sequences for each OTU were aligned using PyNast, with a minimum alignment overlap of 75 bp (16). Alignments were used to build a phylogenetic tree (FastTree (17)). We computed alpha diversity metrics among substrates using the `alpha_diversity.py` script in QIIME (Shannon entropy, species richness, phylogenetic diversity), using the same sequence depth for all samples (3700 sequences per sample). The `beta_diversity_through_plots.py` script was used to compute beta diversity distances between samples (weighted UniFrac), and to construct principal coordinate (PCoA) plots, and account for both the phylogenetic composition (18) and the relative abundance of taxa. Beta-diversity comparisons were done using ANOSIM (`compare_categories.py`; QIIME). We tested whether the abundances of particular OTUs differed significantly between surfaces or sampling times using ANOVA analyses (Bonferonni corrected) with the `otu_category_significance.py` script. ANOVAs and linear regressions were run using the R software package, to compare Shannon diversity to the metadata (19). QIIME was used to calculate the core microbial communities for different surfaces, times, and dates. Taxonomic distributions across sample categories were calculated (from phylum to genus levels) using the `summarize_taxa_through_plots.py` script in QIIME. The 2D histogram of PCoA space was generated using Matplotlib (20).

Quality trimming and de novo metagenome assembly

Raw shot gun sequence reads (paired end; average insert size = 180bp) were quality trimmed using high-throughput sequence analysis toolkit, Neson (<http://www.vicbioinformatics.com/software.nesoni.shtml>) at following parameters; --adaptor-clip, --match 10, --max-errors 1, --clip-ambiguous yes, --quality 10 and --length

70. One of the samples (S1Post25A12pmD3) failed to sequence well, and 94.6% of sequences were lost during quality trimming. The remaining 7 assembly samples were high quality, and only lost 5.6% of their raw reads, on average, during quality filtering. Quality trimmed data from 8 human free samples were assembled into scaffolds using velvet assembler (version 1.2.10) (21) set at following parameters, $k=51$, $-\text{exp_cov}=55$, $-\text{cov_cutoff}=5$, $-\text{ins_length } 180$ $-\text{ins_length_sd } 20$, $-\text{min_contig_lgth}= 250$ and scaffolding=yes. Taxonomical status was assigned to the metagenomes using MetaPhlAn (22).

Metagenome based recovery of genomes

Scaffolds (minimum length = 300bp) from human free metagenome assemblies were clustered into bins using tetra-nucleotide frequency usage anomaly Z-statistics, read depth and %G+C profiles. Briefly, tetra-nucleotide frequency (TNF) based matrix was constructed for each assembly (scaffolds, minimum length = 3kb) using custom R script. TNF values were arcsine square root-transformed before performing clustering via hierarchical agglomerative clustering with squared Euclidean distance and ward criterion in pv-clust package (23) A correlation based (minimum pair-wise R^2 value = 0.9) sub-graph was constructed for each cluster. Each sub-graph was manually checked for read depth and %G+C profiles and outliers ($\text{SEM} \pm 1$) were excluded from further analysis. Taxonomic status was assigned to the reconstructed bins using BLAST2LCA program (<https://github.com/emepyc/Blast2lca>) and phylogenetically divergent contigs were also removed. The completeness of the reconstructed draft genomes ($n=6$) was estimated based on the single copy marker gene profiles (24). Paired end read information was used to iteratively increase the length of draft genomes using the PRICE assembler (25).

Metagenome raw data, assemblies, and reconstructed population genomes were compared against (26) *mecA* (broad-spectrum beta-lactam resistance) and staphylococcal chromosome cassette *mec* (SCC*mec*, mobile genetic element that carries encoded by the *mecA* gene) reference gene sequences using BLASTX. Automated genome annotations of reconstructed *Staphylococcus* population genomes (**Table S1**) were performed using RAST (27) and KAAS (28) servers. A whole genome based maximum likelihood phylogenetic tree was constructed for the reconstructed *Staphylococcus* genomes (**Table S1**) and reference genomes using PhyPhlAn (29).

Data availability

Raw amplicon data is available in the SRA database under accession number SRP049338. 16S and genome assembly raw data, along with sample metadata, can be accessed on FigShare (<http://dx.doi.org/10.6084/m9.figshare.899218>) and MG-RAST-annotated samples can be accessed on the MG-RAST webserver under project number 8313: <http://metagenomics.anl.gov/linkin.cgi?project=8313>.

Results and Discussion

Approximately 14 million high-quality 16S rRNA V4 amplicons representing 77,990 distinct operational taxonomic units (OTUs) were generated from 602 samples, along with bacterial and viral abundance counts. 4.5 million metagenomic reads were sequenced from 7 floor samples for single-read annotation, and 34 million reads were generated from 8 cultured enrichments for genome reassembly.

Longitudinal analysis surface-associated microbial succession

The communities associated with each surface (floor, soap dispenser, and toilet seats) converged upon a confined region within PCoA space within 5 hours following decontamination, and the resulting late-successional surface community structure did not differ significantly across 8 weeks of continued sampling (ANOSIM, $p > 0.8$; **Fig. 2A**, **Fig. 3**). Floor communities showed a rapid reduction in the relative abundances of *Firmicutes* and *Bacteroidetes*, concomitant with a relative increase in the abundances of *Proteobacteria*, *Cyanobacteria* (78.3 % of which are annotated as ‘Chloroplast’, which are likely to be derived from dietary plant biomass (30) or from plant material tracked in from outdoors) and *Actinobacteria* over the course of a day (**Fig. 2B**). Succession was highly reproducible for floor-associated communities, showing equivalent trajectories in four different restrooms over two separate days (**Fig. 3A-C**), and beta-diversity distance was significantly correlated with time (mantel $r = 0.226$, $p < 0.0001$). Floor-associated communities quickly develop toward a meta-stable region within PCoA space (the smaller of the two peaks, **Fig. 2A**; **Fig. 3C**). However, over a slightly longer time frame a more stable optimum is defined by a further reduction in *Firmicutes* and expansion in *Proteobacteria* and *Cyanobacteria* (**Fig. 2**). A Bayesian classifier known as SourceTracker (7), trained on the Earth Microbiome Project (EMP) database (includes both human-associated and environmental samples), showed that the early-successional community is dominated by fecal-associated taxa that are likely aerosolized by toilet flushing (**Fig. 4**), and are largely displaced by skin- and outdoor-associated taxa within 8 hours (**Fig. 2B**; **Fig. 4**). The stable communities present on toilet seats and soap dispensers were comprised of ~45% fecal- and ~45% skin-associated taxa (**Fig. 4**).

Environmental factors influencing surface-associated microbial community structure

Microbial communities clustered significantly based on sample surface (ANOSIM $R = 0.7428$, $p < 0.001$). Only toilet seat samples clustered based on restroom gender (ANOSIM $R = 0.199$, $p = 0.001$; **Fig. 5A**), with *Lactobacillus* and *Anaerococcus* dominating female toilet seats (31-33), and the gut-associated *Roseburia* and *Blautia* being more abundant on male toilet seats (ANOVA, FDR-corrected $p < 0.05$; **Fig. 5B**). High-use and low-use restrooms had significantly different toilet seat and soap dispenser microbial communities (ANOSIM $R = 0.142$, $p = 0.001$, and $R = 0.091$, $p = 0.001$, respectively; **Fig. 5C**), but floor-associated communities were not significantly different. Fecal-associated OTUs were found at a greater relative abundance on high-use toilet seats (e.g. *Bacteroidetes* and *Coproccoccus*), while skin-associated OTU were more prevalent on low-usage seats (e.g. *Corynebacterium*; **Fig. 5D**).

Changes in community structure after human-exclusion

In the eight hours following the exclusion of humans there was no significant reduction in the prevalence of fecal microbiota (Pearson's $R = -0.1093$; $p = 0.45$). This persistence of fecal microbiota, as in the late-successional floor community, is potentially due to dormant or endospore forming taxa (e.g. *Firmicutes*; **Fig. 2B**). We suggest that active fecal microbiota would experience a significant shock when transiting between the warm, moist, anaerobic conditions of the host to the colder, drier, aerobic floor. Thus, we propose that fecal taxa able to enter into a dormant phase can persist for longer periods of time on restroom surfaces, although further work needs to be done to quantify dormancy in these BE systems. The floor community structure, following human exclusion, resembled the late-successional floor communities, while the viable organisms that grew in culture from these same samples resembled a subset of soap dispenser and toilet-seat

associated communities (weighted Unifrac; **Fig. S2**). These viable communities were not significantly different across time or between culture conditions (i.e. anaerobic or aerobic, at 25° or 37° C; weighted UniFrac; ADONIS, $p > 0.8$). Despite the lack of statistical difference in beta-diversity between culture conditions, we did see notable differences in the source environments. Skin- and outdoor-associated taxa comprised 68-98%, and fecal taxa represented 0-15% of the cultured communities. On average, both pre- and post-culture communities had a larger percentage of outdoor-associated taxa than other samples from the prior experiments, which suggests that, over time, human-associated taxa are displaced in the absence of dispersal (**Fig. 4**). Looking specifically at different culture conditions, ambient temperature (25°C), under both aerobic and anaerobic culture conditions, showed equal proportions of environmental- and skin-associated taxa in the cultures (~1:1). However, at human body-temperature (37°C), skin-associated microbiota were dominant (~70% of the community), regardless of oxygen potential. Several *Staphylococcus* taxa were positively correlated with incubation temperature (Bonferroni-corrected Pearson's $p < 0.05$), and several OTUs shared 100% nucleotide similarity across the 16S rRNA V4 region with *Staphylococcus aureus*, which is the most common cause of skin and soft tissue infections (34). The presence of *Staphylococcus* isolates was verified by metagenome assembly of several pan-genomes from cultured samples (**Fig. 6, Table S1**), which shows that opportunistic pathogens remain viable on surfaces for many hours following human exclusion. The assembled pan-genomes made up large fractions of the total number of shotgun reads from most of sequenced culture metagenomes (**Table S2**). **Table S3** shows the distribution of annotated genes across SEED subsystem functional categories for each pan-genome.

Composition of the surface-associated core microbial community

Of the taxa that were ubiquitous across samples, most were associated with phyla that are known to dominate the human gut (except for *Corynebacterium*). While skin-associated OTUs dominated overall, they were not represented in this core community, because they were likely derived from a more diverse seed bank, as the human skin microbiome is more variable through time than the gut (35). Concordantly, Shannon diversity rises significantly from morning to afternoon (in the 8-hour study), which supports the idea that late-successional taxa are derived from more diverse sources ($R^2 = 0.282$, $p < 0.0001$; **Fig. S3A**).

Viral:bacterial ratios and the composition of the viral metagenome

Bacterial and viral abundances, as determined by epifluorescence microscopy, were significantly positively correlated ($R = 0.764$, $p < 0.0001$; **Fig. S3B**), and were negatively correlated with temperature ($R^2 = 0.048$ and $R^2 = 0.153$, respectively; $p < 0.03$). Bacterial abundance was positively, albeit weakly, correlated with humidity ($R^2 = 0.0412$, $p < 0.02$). Viral abundance was significantly lower in high-usage restrooms (ANOVA, $p < 0.002$), but no significant relationship existed between either viral or bacterial abundance and gender. Absolute viral and bacterial abundance show no discernable trend across time, as the bacterial community reaches an abundance plateau ($\sim 6.2 \times 10^3$ cells cm^{-2} , as determined by microscopy) within 1 hour after decontamination, suggesting limited growth and a high rate of dispersal. The viral:bacterial (v:b) ratio was $\sim 1:1$, which is around 10-20 times lower than considered typical for environmental samples (36). We speculate that this lowered ratio suggests microbial dormancy (e.g., sporulation, persister cells, or lowered metabolic rates) as phage lytic cycles cannot occur

in dormant cells. Even if lytic cycles could occur, the low bacterial density observed on these surfaces may further limit the spread of phage (37).

In the human-exclusion experiment, v:b ratios tended to be lower (0.2-0.3). The ratios differed across culture conditions as well (aerobic at 25° C = 0.204 ± 0.253 SD; anaerobic at 25° C = 0.040 ± 0.006 SD; aerobic at 37° C = 0.211 ± 0.131 SD; and anaerobic at 37° C = 0.338 ± 0.151 SD). Most of the phage detected on restroom surfaces were enterophages (within *Microviridae*; **Fig. S4**), and because there were few gut microbes that persisted on surfaces, or that grew up in culture, it follows that phage abundance would remain low in the absence of their hosts. The fact that the 25° C, anaerobic condition consistently yielded the lowest v:p ratio may indicate that most phage/hosts are unlikely to have encountered this condition in their original environmental context (e.g. the anaerobic gut environment is at 37° C, and non-host associated environments that are likely to be dispersal sources for restrooms, like soils, tend to be aerobic). The most abundant viral group within *Microviridae* was enterophage ϕ X174, indicating that most of the viral sequences detected on restroom surfaces were derived from the gut. Human papilloma viruses (within the *Papillomaviridae* family) and human herpes viruses (within *Herpesvirales*) were also detected in high abundance, which are skin- and epithelium-associated (38, 39).

Metagenome data show the prevalence of bacterial virulence factors

In addition to standard cellular functions such as carbohydrate and protein metabolism (**Fig. S5A**), virulence-associated functions were present, including fluoroquinolone resistance, heavy metal efflux and multidrug efflux pumps (**Fig. S5B**). *Staphylococcus* methicillin-resistance pathways were the 6th most abundant category

(representing 3% of ‘Bacterial’ sequences; **Fig. S5C**). *S. aureus* is increasing in prevalence outside of the hospital environment (34), and these results suggest that it might be a common constituent of public restroom surfaces. Culturing work showed a high prevalence of Staphylococcal species, but the assembled pan-genomes of cultured organisms did not contain methicillin-resistance genes.

Conclusion

When compared to host-associated environments, restroom surfaces are dry, barren, and resource-poor. As such, these surfaces probably do not support considerable microbial growth, as evidenced by low cell densities. Continual dispersal, dormancy, and cell death appear to be the dominant forces shaping community structure through time, with minor contributions from cell growth and competition. The prevalence of skin-associated, rather than fecal-associated taxa, in the late-successional community suggests that organisms are selected for their ability to persist in a dry, aerobic environment, which is a very different environment from the gut. Human-associated microbiota, including *Staphylococcus* strains, can remain viable on BE surfaces for many hours after their dispersal agents are removed. This suggests that common BE surfaces may be significant fomites for viable human pathogens.

Acknowledgements

S.M.G. was supported by an EPA STAR Graduate Fellowship and the National Institutes of Health Training Grant 5T-32EB-009412. We acknowledge funding from the Alfred P Sloan Foundation’s Microbiology of the Built Environment Program. This work was completed in part with resources provided by the University of Chicago Research Computing Center.

We would like to thank Sarah Owens and Jarrad Hampton-Marcell at Argonne National Laboratory for help with DNA extraction, amplification, and sequencing. Thanks to Reto Trappitsch for help with Matplotlib and Maureen L. Coleman for helpful discussion. We would also like to thank Julia Bell for her help with study organization and planning.

References

1. **Custovic A, Taggart S, Woodcock A.** 1994. House dust mite and cat allergen in different indoor environments. *Clin Exp Allergy* **24**:1164.
2. **Kelley ST, Gilbert JA.** 2013. Studying the microbiology of the indoor environment. *Genome Biol* **14**:1-9.
3. **Kembel SW, Jones E, Kline J, Northcutt D, Stenson J, Womack AM, Bohannan BJ, Brown G, Green JL.** 2012. Architectural design influences the diversity and structure of the built environment microbiome. *ISME J* **6**:1469-1479.
4. **Flores GE, Bates ST, Knights D, Lauber CL, Stombaugh J, Knight R, Fierer N.** 2011. Microbial Biogeography of Public Restroom Surfaces. *PLoS One* **6**:e28132.
5. **Rintala H, Pitkäranta M, Toivola M, Paulin L, Nevalainen A.** 2008. Diversity and seasonal dynamics of bacterial community in indoor environment. *BMC Microbiol* **8**:56.
6. **Angenent LT, Kelley ST, Amand AS, Pace NR, Hernandez MT.** 2005. Molecular identification of potential pathogens in water and air of a hospital therapy pool. *P Natl Acad Sci USA* **102**:4860-4865.
7. **Knights D, Kuczynski J, Charlson ES, Zaneveld J, Mozer MC, Collman RG, Bushman FD, Knight R, Kelley ST.** 2011. Bayesian community-wide culture-independent microbial source tracking. *Nat Methods* **8**:761-763.
8. **Hewitt KM, Gerba CP, Maxwell SL, Kelley ST.** 2012. Office space bacterial abundance and diversity in three metropolitan areas. *PLoS One* **7**:e37849.
9. **Knight R, Jansson J, Field D, Fierer N, Desai N, Fuhrman JA, Hugenholtz P, van der Lelie D, Meyer F, Stevens R.** 2012. Unlocking the potential of metagenomics through replicated experimental design. *Nat Biotechnol* **30**:513-520.
10. **Sano E, Carlson S, Wegley L, Rohwer F.** 2004. Movement of viruses between biomes. *Appl Environ Microb* **70**:5842-5846.
11. **Caporaso JG, Lauber CL, Walters WA, Berg-Lyons D, Huntley J, Fierer N, Owens SM, Betley J, Fraser L, Bauer M, Gormley N, Gilbert JA, Smith G, Knight R.** 2012. Ultra-high-throughput microbial community analysis on the Illumina HiSeq and MiSeq platforms. *ISME J* **6**:1621-1624.

- 479 12. **Glass EM, Meyer F.** 2011. The Metagenomics RAST Server: A Public Resource
480 for the Automatic Phylogenetic and Functional Analysis of Metagenomes, p. 325-
481 331, Handbook of Molecular Microbial Ecology I. John Wiley & Sons, Inc.
- 482 13. **Caporaso JG, Kuczynski J, Stombaugh J, Bittinger K, Bushman FD, Costello**
483 **EK, Fierer N, Pena AG, Goodrich JK, Gordon JI, Huttley GA, Kelley ST,**
484 **Knights D, Koenig JE, Ley RE, Lozupone CA, McDonald D, Muegge BD,**
485 **Pirrung M, Reeder J, Sevinsky JR, Turnbaugh PJ, Walters WA, Widmann**
486 **J, Yatsunenko T, Zaneveld J, Knight R.** 2010. QIIME allows analysis of high-
487 throughput community sequencing data. *Nat Meth* **7**:335-336.
- 488 14. **Rideout JR, He Y, Navas-Molina JA, Walters WA, Ursell LK, Gibbons SM,**
489 **Chase J, McDonald D, Gonzalez A, Robbins-Pianka A.** 2014. Subsampled
490 open-reference clustering creates consistent, comprehensive OTU definitions and
491 scales to billions of sequences. *PeerJ* **2**:e545.
- 492 15. **McDonald D, Price MN, Goodrich J, Nawrocki EP, DeSantis TZ, Probst A,**
493 **Andersen GL, Knight R, Hugenholtz P.** 2012. An improved Greengenes
494 taxonomy with explicit ranks for ecological and evolutionary analyses of bacteria
495 and archaea. *ISME J* **6**:610-618.
- 496 16. **Caporaso JG, Bittinger K, Bushman FD, DeSantis TZ, Andersen GL, Knight**
497 **R.** 2010. PyNAST: a flexible tool for aligning sequences to a template alignment.
498 *Bioinformatics* **26**:266-267.
- 499 17. **Price MN, Dehal PS, Arkin AP.** 2010. FastTree 2 – Approximately Maximum-
500 Likelihood Trees for Large Alignments. *PLoS One* **5**:e9490.
- 501 18. **Lozupone C, Knight R.** 2005. UniFrac: a New Phylogenetic Method for
502 Comparing Microbial Communities. *Appl Environ Microb* **71**:8228-8235.
- 503 19. **R Core Development Team.** 2008. R: A language and environment for statistical
504 computing. R Foundation for Statistical Computing, Vienna, Austria.
- 505 20. **Hunter JD.** 2007. Matplotlib: A 2D graphics environment. *Comput Sci Eng* **90**-
506 **95**.
- 507 21. **Zerbino DR, Birney E.** 2008. Velvet: algorithms for de novo short read assembly
508 using de Bruijn graphs. *Genome Res* **18**:821-829.
- 509 22. **Haft DH, Tovchigrechko A.** 2012. High-speed microbial community profiling.
510 *Nat Methods* **9**:793-794.
- 511 23. **Suzuki R, Shimodaira H.** 2006. Pvcult: an R package for assessing the
512 uncertainty in hierarchical clustering. *Bioinformatics* **22**:1540-1542.
- 513 24. **Wu M, Scott AJ.** 2012. Phylogenomic analysis of bacterial and archaeal
514 sequences with AMPHORA2. *Bioinformatics* **28**:1033-1034.
- 515 25. **Ruby JG, Bellare P, DeRisi JL.** 2013. PRICE: software for the targeted
516 assembly of components of (meta) genomic sequence data. *G3* **3**:865-880.
- 517 26. **Elements IWGotCoSCC.** 2009. Classification of staphylococcal cassette
518 chromosome mec (SCCmec): guidelines for reporting novel SCCmec elements.
519 *Antimicrob Agents Ch* **53**:4961-4967.
- 520 27. **Aziz RK, Bartels D, Best AA, DeJongh M, Disz T, Edwards RA, Formsma K,**
521 **Gerdes S, Glass EM, Kubal M.** 2008. The RAST Server: rapid annotations using
522 subsystems technology. *BMC Genomics* **9**:75.

28. **Moriya Y, Itoh M, Okuda S, Yoshizawa AC, Kanehisa M.** 2007. KAAS: an automatic genome annotation and pathway reconstruction server. *Nucleic Acids Res* **35**:W182-W185.
29. **Segata N, Börnigen D, Morgan XC, Huttenhower C.** 2013. PhyloPhlAn is a new method for improved phylogenetic and taxonomic placement of microbes. *Nat Commun* **4**.
30. **Kelley ST, Dobler S.** 2011. Comparative analysis of microbial diversity in Longitarsus flea beetles (Coleoptera: Chrysomelidae). *Genetica* **139**:541-550.
31. **Vásquez A, Jakobsson T, Ahrné S, Forsum U, Molin G.** 2002. Vaginal Lactobacillus flora of healthy Swedish women. *J Clin Microbiol* **40**:2746-2749.
32. **Ma B, Forney LJ, Ravel J.** 2012. Vaginal microbiome: rethinking health and disease. *Annu Rev Microbiol* **66**:371-389.
33. **Ravel J, Gajer P, Abdo Z, Schneider GM, Koenig SS, McCulle SL, Karlebach S, Gorle R, Russell J, Tacket CO.** 2011. Vaginal microbiome of reproductive-age women. *P Natl Acad Sci USA* **108**:4680-4687.
34. **LeBlanc DM, Reece EM, Horton JB, Janis JE.** 2007. Increasing incidence of methicillin-resistant Staphylococcus aureus in hand infections: a 3-year county hospital experience. *Plast Reconstr Surg* **119**:935-940.
35. **Costello EK, Lauber CL, Hamady M, Fierer N, Gordon JI, Knight R.** 2009. Bacterial community variation in human body habitats across space and time. *Science* **326**:1694-1697.
36. **Weinbauer MG.** 2004. Ecology of prokaryotic viruses. *FEMS Microbiol Rev* **28**:127-181.
37. **Lewis K.** 2010. Persister cells. *Annu. Rev. Microbiol.* **64**:357-372.
38. **Davison AJ, Eberle R, Ehlers B, Hayward GS, McGeoch DJ, Minson AC, Pellett PE, Roizman B, Studdert MJ, Thiry E.** 2009. The order herpesvirales. *Arch Virol* **154**:171-177.
39. **Walboomers JM, Jacobs MV, Manos MM, Bosch FX, Kummer JA, Shah KV, Snijders PJ, Peto J, Meijer CJ, Munoz N.** 1999. Human papillomavirus is a necessary cause of invasive cervical cancer worldwide. *J Pathol* **189**:12-19.

Figure Legends

Figure 1. (A) Samples were collected from three surfaces in both female and male restrooms at San Diego State University. The surfaces analyzed were the toilet seat, the floor in front of the toilet, and the soap dispenser pump. Epifluorescence microscopy confirmed that bacteria and virus like particles (VLPs) are present on all three surfaces. (Restroom cartoon modified from Flores et al., 2011). (B) Epifluorescence microscopy images show selected restroom surfaces are DNA and RNA free after twenty minutes of treatment with 10% bleach; T is the length of time the surface was soaked in bleach.

Figure 2. (A) A 2D histogram of floor samples (including 8-hour, 8-week, and month-long experiments) in principal coordinate space (weighted UniFrac). Peaks denote areas within principal coordinate space where samples are found most frequently (regions of stability). The smaller peak corresponds to the later time points in the 8-hour study. The

larger peak shows the stable community state that remains relatively fixed in the 9-week and month-long samplings (corresponding to the community structures highlighted in red in panel B). We only observed early-successional community composition in the 8-hour time series. Over longer timescales, the community was consistently found in the late-successional state. (B) Composition of the microbial community along its successional trajectory. The asterisk above the 8AM time point denotes the sample taken directly following rigorous decontamination of the floor surface with bleach. The orange and red boxes surrounding time points refer to the average community states characteristic of the two peaks (labeled with corresponding colors: orange and red) seen in panel A.

Figure 3. PCoA plots of floor microbial communities over different timescales. (A) Replicate 8-hour time series experiments cluster on top of one another. (B) Same plot as in (A), but with samples colored by time point, and time point replicates encapsulated by convex hulls. (C) Samples from the 8-hr experiment (rainbow colors) show a larger spread than samples taken from longer-term studies (8-week and 1-month with daily sampling; dark blue), showing that succession is rapid and occurs within 5-8 hours. Black arrow in panel C shows the successional trajectory.

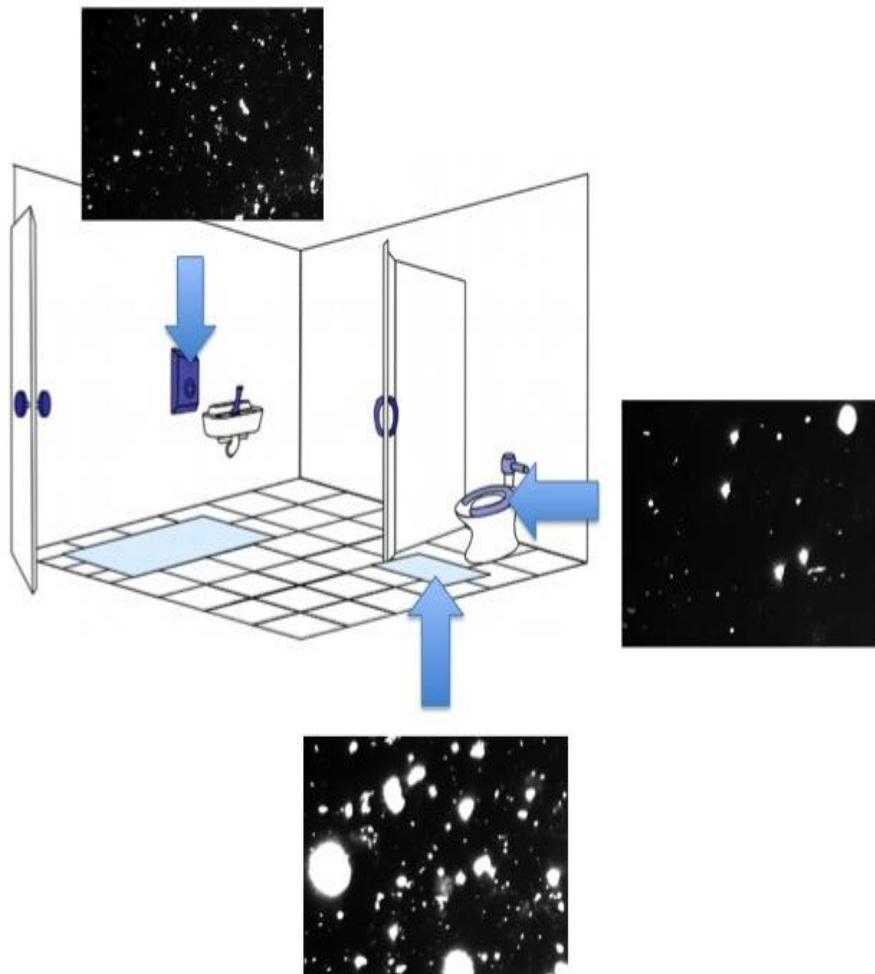
Figure 4. The relative proportion of OTUs derived from particular source environments (as determined using SourceTracker). The first eight samples represent the average of replicates taken at each hour for the 8-hour study. The 8-week and month bars represent the average of all replicates for floor samples only. Soap and seat bars show the average of replicates for those surfaces across the 8-week and month-long studies. The pre- and post-culture bars represent the averages from the human-exclusion study (floor samples prior to culturing, and after culturing). The asterisk above the 8AM bar indicates that the floor was decontaminated prior to taking this sample. The source environment database was constructed using Earth Microbiome Project (EMP) data (closed reference OTUs; Greengenes release from May, 2013). The ‘outdoor’ category includes database samples from many outdoor environments: freshwater, freshwater microbial mat, freshwater sediment, bird nest, hot springs water, hot springs microbial mat, ice, marine biofilm, marine water, marine sediment, hypersaline water, sand, sandstone, soil.

Figure 5. PCoA (weighted UniFrac) in (A) shows a clear separation of toilet seat associated microbial communities based on gender. (B) depicts the top 10 most abundant OTUs that show significant differences in abundance between male and female toilet seats (most resolved taxonomic annotation shown on x-axis). (C) shows seat samples cluster separately based on restroom usage frequency (high vs. low). (D) displays 7 OTUs that exhibit significantly different abundances between high and low usage frequencies (most resolved taxonomic annotations are listed along x-axis).

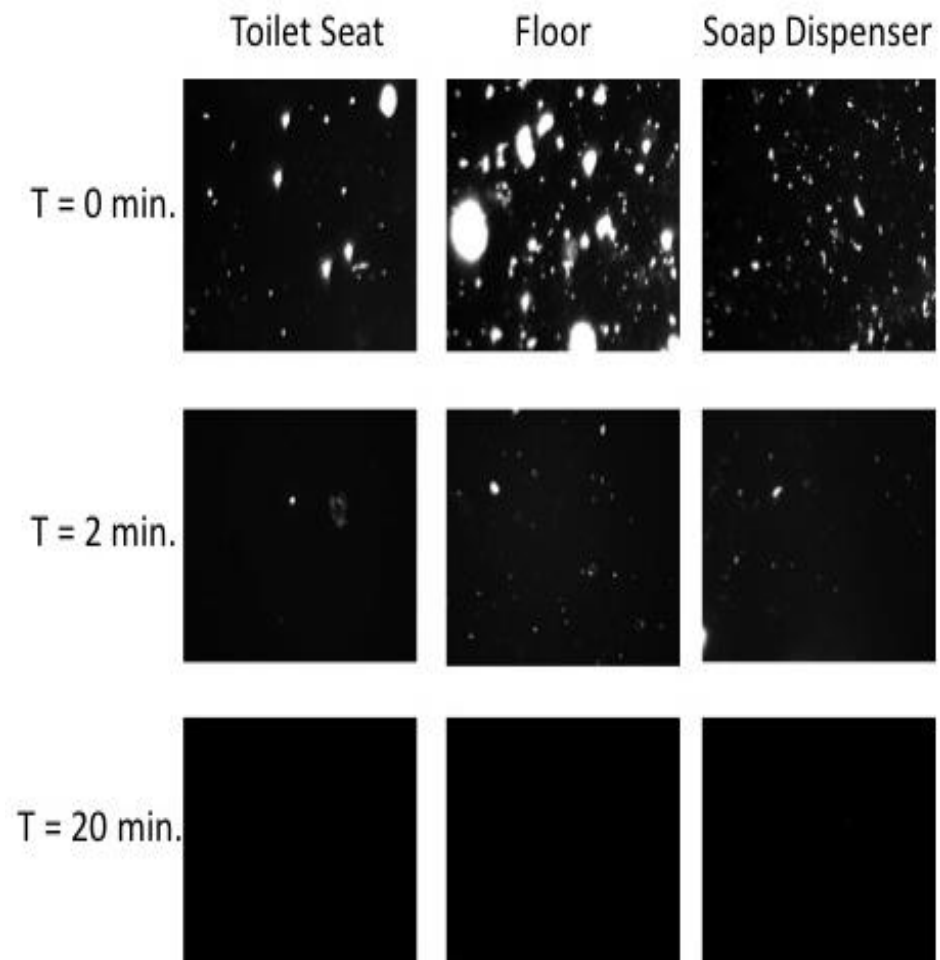
Figure 6. Species-level metagenomic diversity from metagenomic assemblies of post-culture swab samples, from the human free study. (A) species-level (SK1-SK8) relative abundance patterns across 8 metagenomes, with hierarchical clustering of both rows and columns (average linkage clusters, using Bray-Curtis distance), reporting only the 25 most abundant species annotations (according to the 90th percentile of the abundances). The heatmap key shows percent relative abundance. (B) Rooted tree representing the

614 phylogenetic position of 6 *Staphylococcus* population genomes (highlighted in blue),
615 along with reference strains and *Bdellovibrio bacteriovorus HD100* as the out-group. The
616 tree was constructed using PhyloPhlAn (29) with concatenated amino acid sequences
617 from ~400 conserved proteins. Values assigned to internal nodes within the phylogeny
618 represent bootstrap support (bootstrap values < 0.50 are not reported). The scale bar
619 represents 0.2 changes per amino acid position.
620

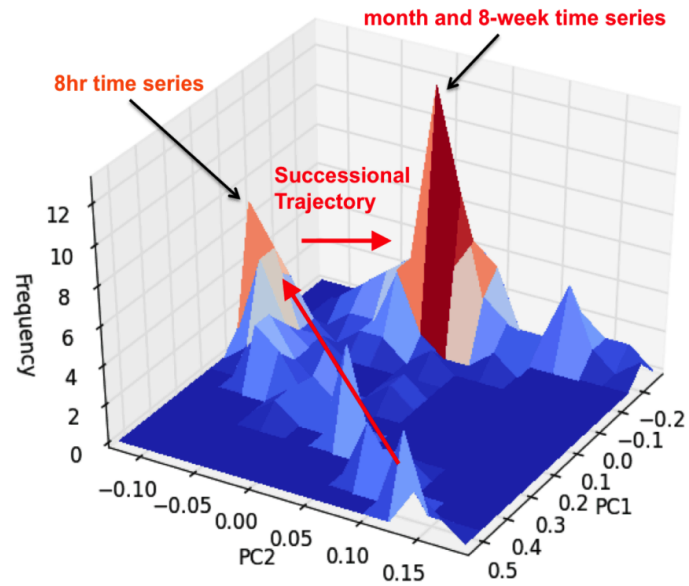
A.



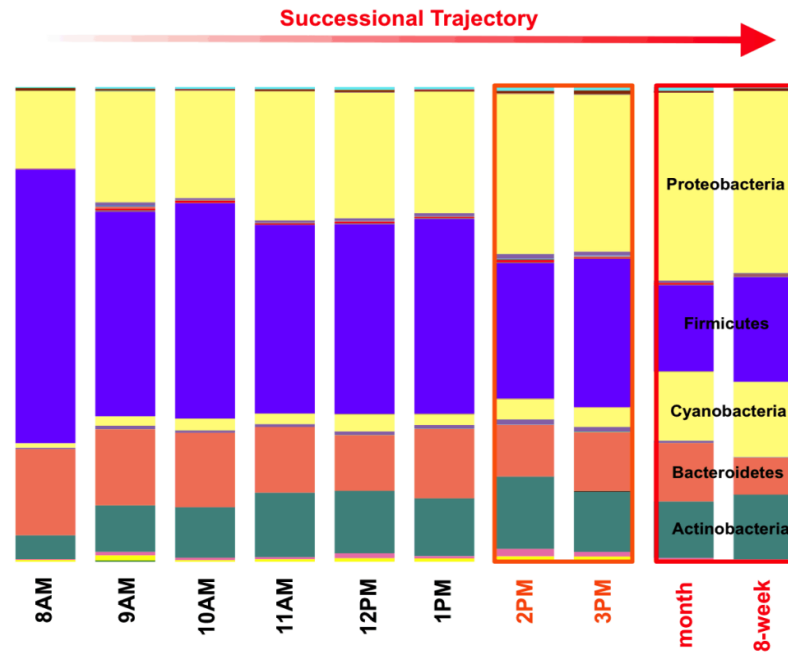
B.

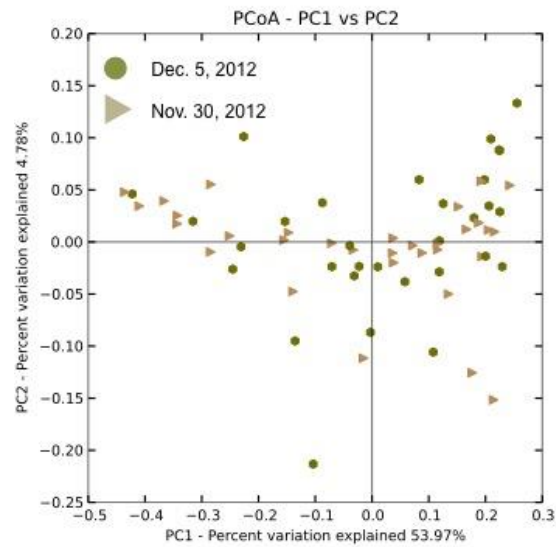
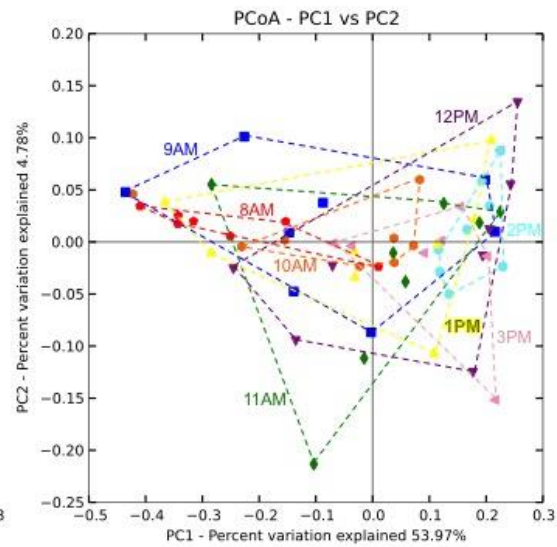
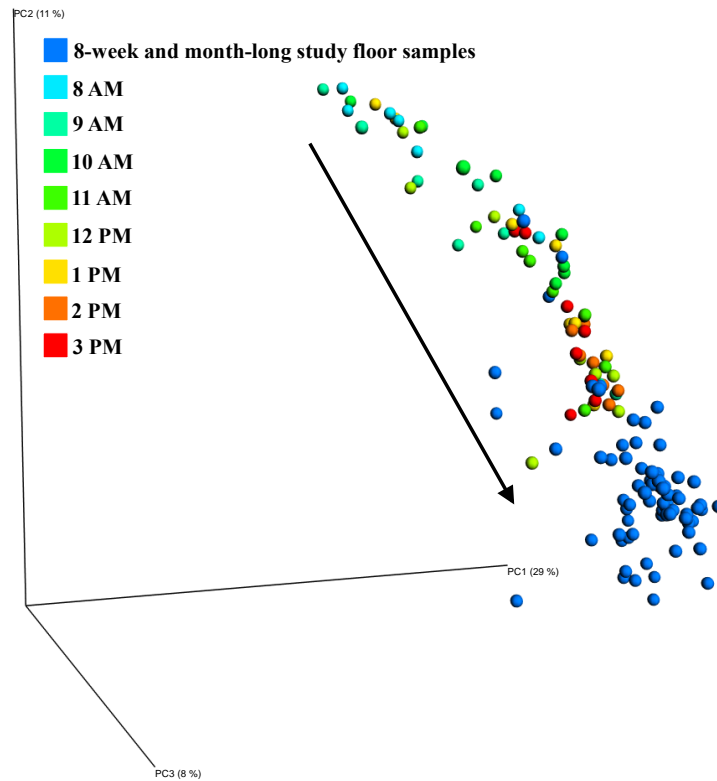


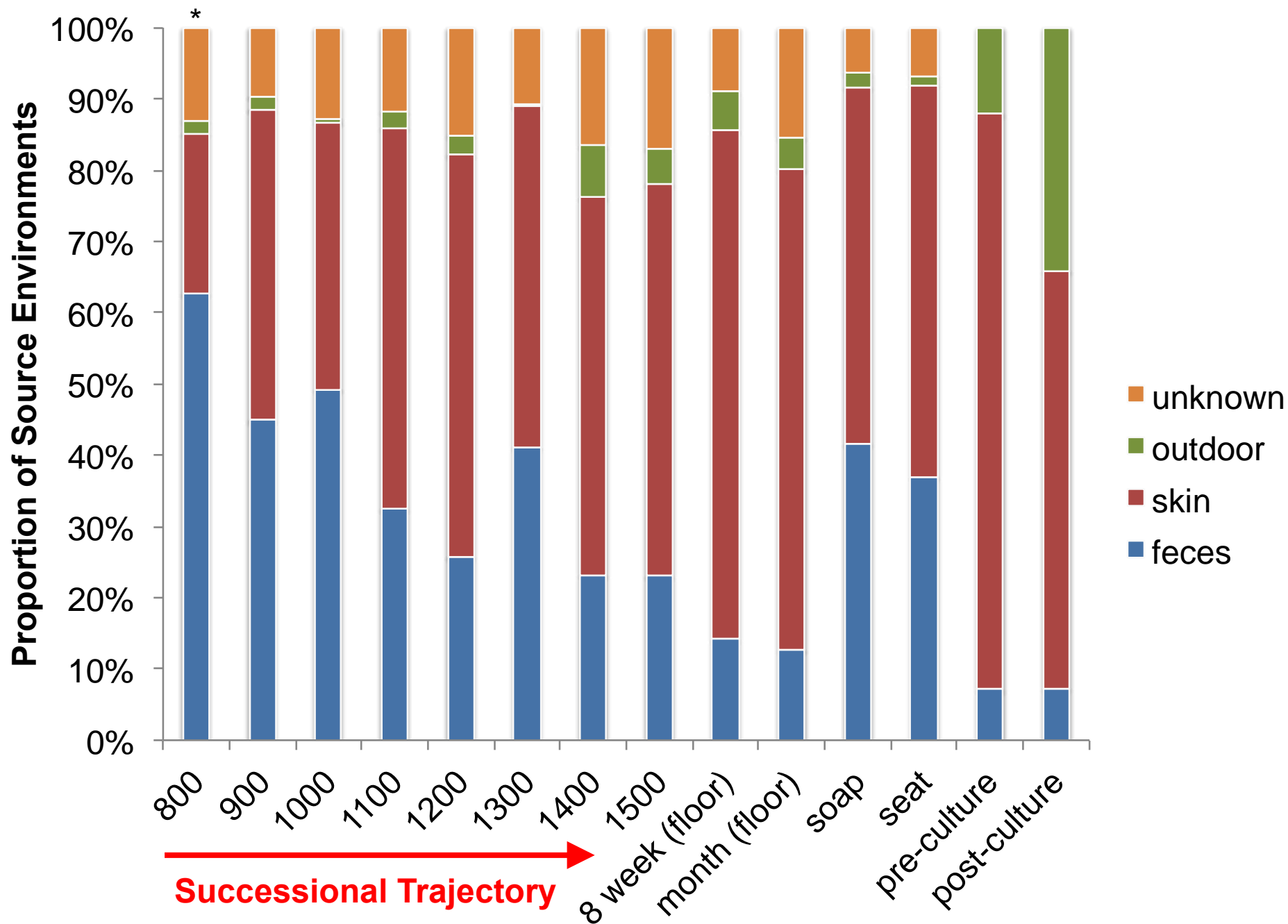
A.

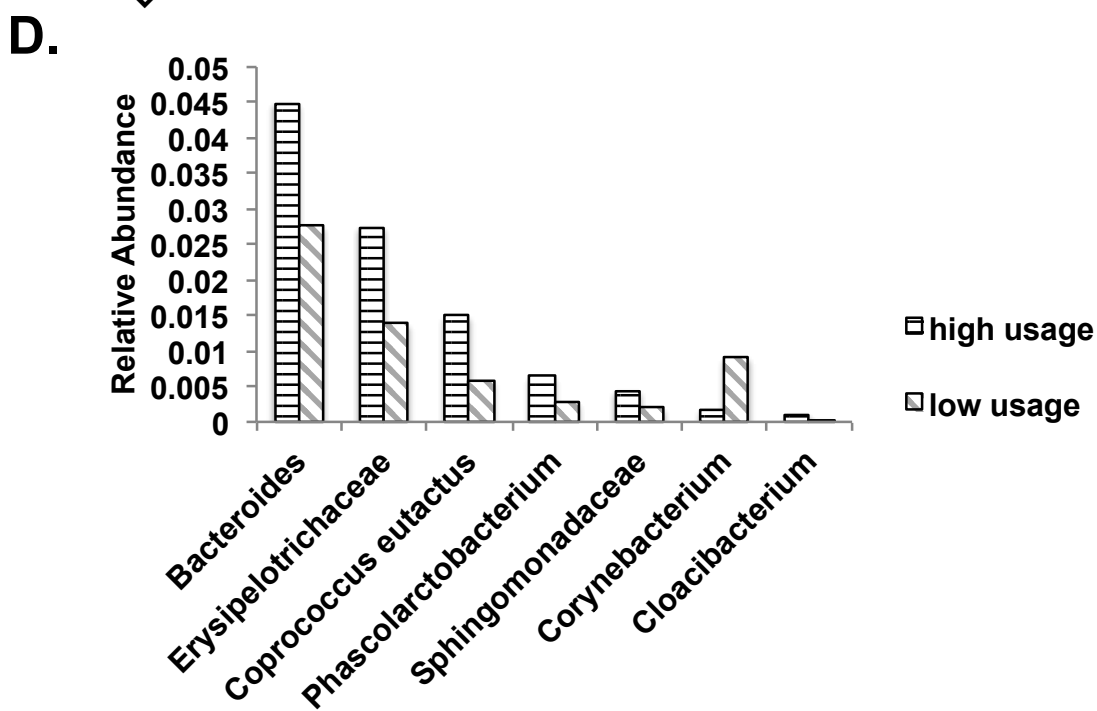
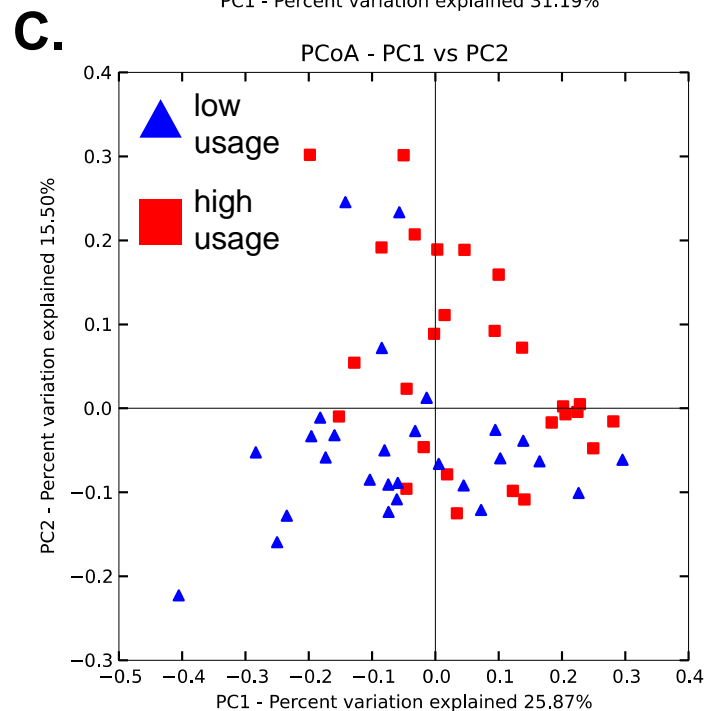
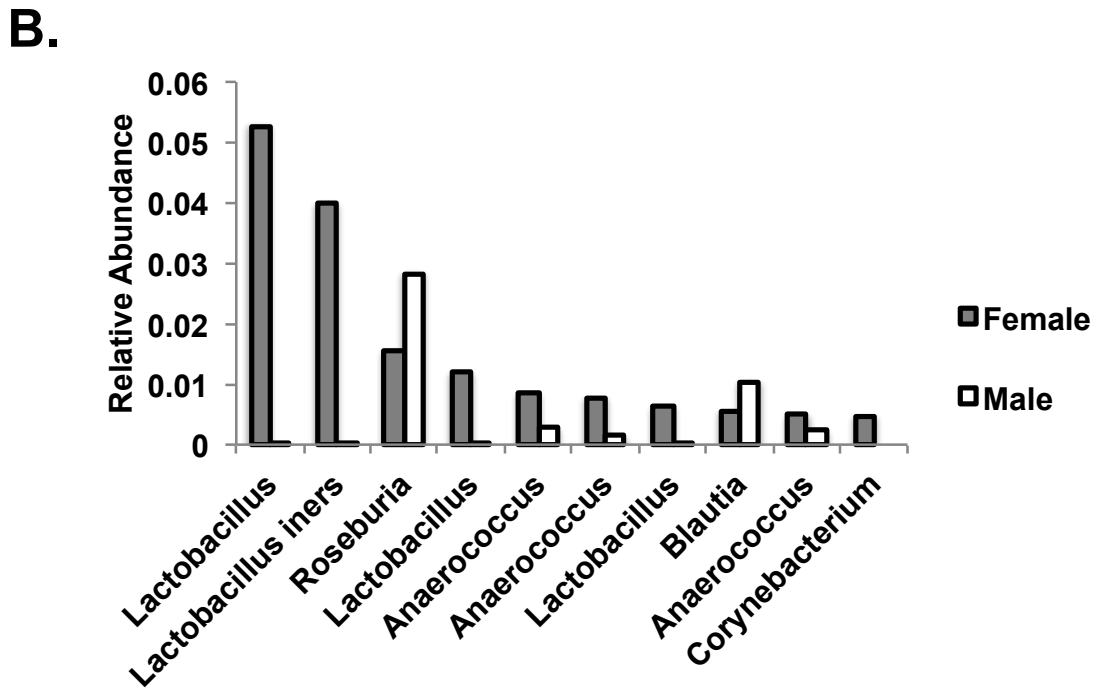
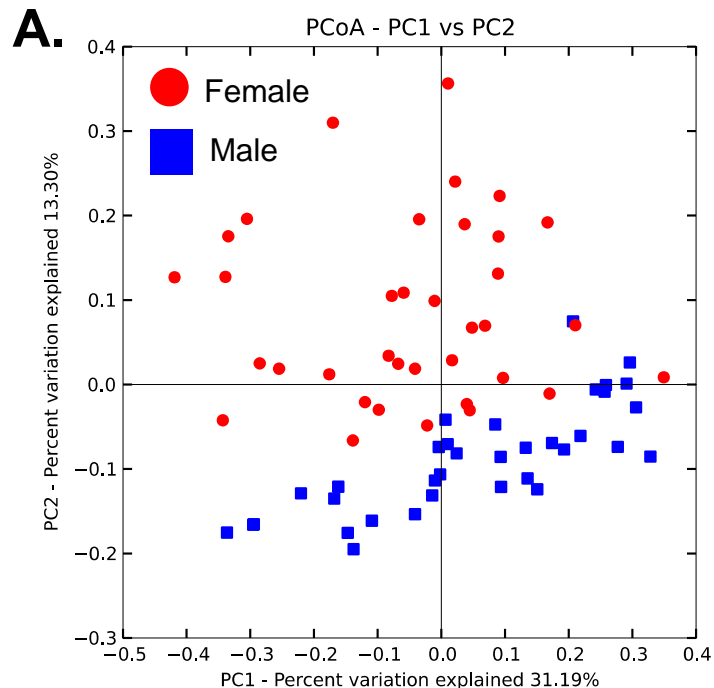


B.

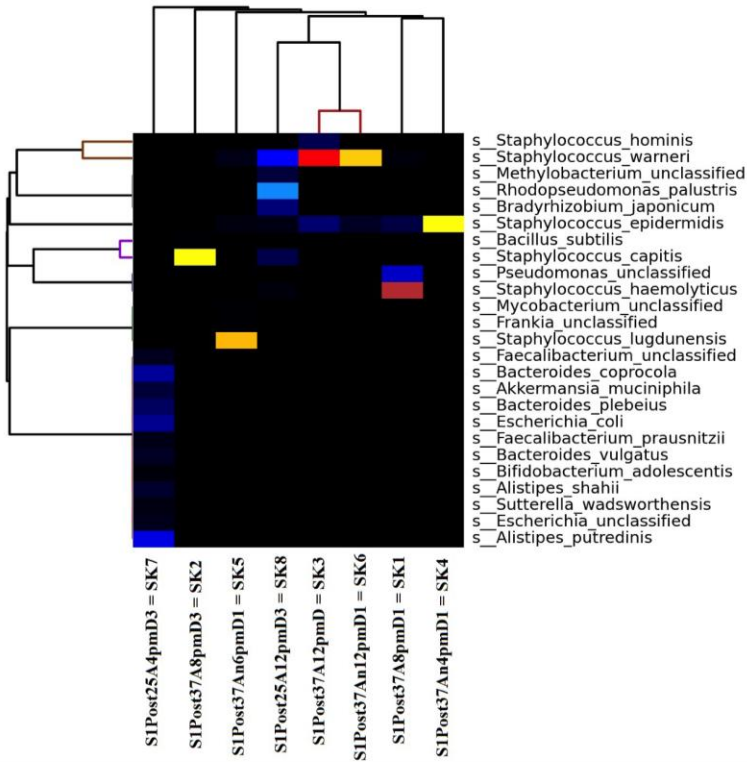


A.**B.****C.**





A horizontal color scale bar with numerical labels 10, 20, 30, 40, 50, 60, 70, 80, and 90. The colors transition from dark blue at 10, through light blue, cyan, green, yellow, and orange, to red at 90.



B.

